SLAC-PUB-15172

FEEDBACK REQUIREMENTS FOR SASE-FELs*

H. Loos†, SLAC, Menlo Park, CA 94025, USA

Abstract

The operation of a SASE FEL at soft and hard X-ray wavelengths driven by a high brightness electron beam imposes strong requirements on the stability of the accelerator and feedback systems are necessary to both guarantee saturation of the SASE process as well as a stable photon beam for user experiments. Diagnostics for the relevant transverse and longitudinal beam parameters are presented and various examples of feedback systems for bunches with low repetition rate as well as systems for intra bunch train feedbacks are discussed.

INTRODUCTION

The development of Self Amplified Spontaneous Emission (SASE) Free Electron Lasers (FEL) operating from EUV [1, 2] down to Angstrom wavelengths [3] sets more and more stringent requirements for the stability of the electron beam parameters and hence the beam feedback systems and their related diagnostics. The main electron beam and undulator parameters of the operating X-Ray FEL project LCLS and the XFEL/SPring-8 [4] and E-XFEL [5] projects under construction are given in Table 1.

Table 1: X-Ray SASE FEL Projects

	LCLS	SCSS	XFEL
Repetition rate (Hz)	120	60	10
Bunch train rate (MHz)	-	-	5
Energy (GeV)	13.6	8	17.5
X-ray wavelength (nm)	0.15	0.1	0.1
Charge (nC)	0.25-1	0.3	0.1-1
Bunch length (μm)	8-20	25	20
Peak current (kA)	3.4	5	2.5
Undulator length (m)	100	100	130
Undulator β (m)	30	30	32
Beam size (μm)	30	45	35
3-D Gain length (m)	3.5	3.7	10

The common features of all projects operating at 1 Å are an injector providing electron bunches with charge of up to 1 nC and energy at the 100 MeV level, subsequent acceleration sections to several GeV with two magnetic bunch compressor chicanes in between to reach peak currents of several kA, and an undulator magnet system of typically 100 m lengths to achieve saturation within 10 to 20 gain lengths of about 3 to 10 meters. The transverse and longitudinal feedback systems have to achieve two goals. One is to provide sufficient stability of the beam parameters to enable saturation of the SASE process within the length of the undulator and the other is to provide a photon beam which satisfies the requirements of the user experiments in terms of wavelength, pointing, and timing stability.

The main transverse requirement for efficient SASE gain is given by a limit on the beam angle in the undulator such that the phase difference due to the longer beam path remains a fraction of the wavelength. The critical angle where the SASE gain length L_{G} vanishes is given by [6] $\theta_c = \sqrt{\lambda/L_{\mathrm{G}}}$. With typical parameters taken from Table 1 this means that the orbit angle has to be stable within a fraction of $\theta_c = 5\,\mu$rad. The stable pointing of the photon beam is usually defined as a requirement of $\sigma/10$ for the electron beam position in terms of the rms beam size σ. This means less than $5\,\mu$m rms position jitter for a $1\,\mu$m emittance beam in an undulator with typically 30 m β-function.

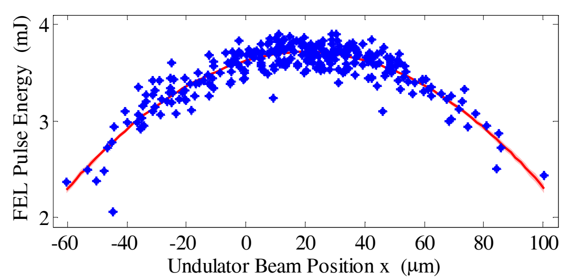

Figure 1: Sensitivity of LCLS FEL pulse energy on beam position in the undulator at 6.7 GeV. The red line is a Gaussian fit with $\sigma = 90\,\mu$m.

The effect of orbit jitter on the SASE performance can be seen in Fig. 1 which shows the FEL pulse energy vs. the horizontal beam position in the undulator for 300 shots. The orbit jitter was mainly from uncorrected dispersion in the undulator when the accelerator was not fully optimized. The FWHM of the fit corresponds to a critical angle of $15\,\mu$rad which agrees well with the theoretical value.

The requirements for the longitudinal beam parameters can all be derived from the dimensionless FEL efficiency parameter ρ which is of the order of 10^{-4} for an X-ray FEL. The bandwidth of the photon beam is of the same order which requires an energy stability of 10^{-4} for a stable X-ray wavelength. The energy stability also affects the stability of the arrival time of the photon beam because the energy jitter introduces a timing jitter in the bunch compressor chicanes of approximately $c\Delta t = R_{56}\Delta E/E$, which amounts to 10s of fs for R_{56} of several cm. If the beam energy is measured from the beam position in the chicane, the 10^{-4} energy stability translates into a $10\,\mu$m position

* Work supported by US DOE contract DE-AC02-76SF00515.
† loos@slac.stanford.edu

resolution assuming a typical dispersion of 10 cm. Alternatively, the energy can be obtained from a time of flight measurement between bunch arrival monitors (BAM) before and after the chicane.

For normal conducting accelerators operating at about 100 Hz repetition rate, a feedback system can only control slow drifts at much smaller frequencies and shot to shot jitter has to be minimized at the respective source. Superconducting accelerators can be operated with long bunch trains with sub-μs bunch spacing at a repetition rate of 10s of Hz. This requires besides the slow macro-pulse feedback also a fast intra-bunch feedback (IBFB) to correct disturbances within the bunch train.

The following sections discuss both diagnostics and implementations for transverse and longitudinal feedback systems at various SASE FEL projects.

TRANSVERSE FEEDBACK

The necessity of orbit straightness and stability to a few μm in the undulator to achieve sufficient SASE gain and of the more general goal of orbit stability at the $\sigma/10$ level in the accelerator requires BPMs with resolutions at the same level to be used in transverse feedback systems.

Transverse Diagnostics

Sub-micron resolution for the undulator can be met with RF cavity BPMs and one of a few μm with strip line BPMs. The performance of both types at the LCLS is shown in Fig. 2 for a total of 150 BPMs using the correlations between the BPMs for 500 beam pulses.

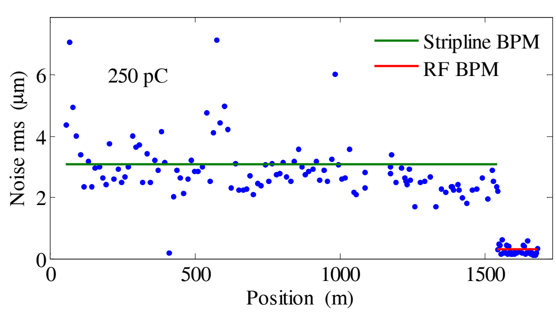

Figure 2: LCLS strip-line and RF cavity BPM noise levels.

The average noise for the strip line BPMs is about 3 μm. The long term stability of the strip line BPMs which is important for the transverse feedback is reached by applying calibration pulses to the electrodes between beam pulses [7]. Sub-micron resolution is achieved for the undulator BPMs with a RF cavity BPM design [8] operating at X-band frequency of 11.4 GHz. It consists of a dipole cavity and a monopole cavity used for signal normalization. The BPMs have to be calibrated using signals from the beam itself by either moving the BPM cavity or by inducing known orbit oscillations. Long term BPM offset drifts have to be adjusted by regularly finding the absolute BPM centers with an undulator beam based alignment procedure [9]. The resolution was measured to about 300 nm [10] at the normal operating charge of 250 pC.

The cavity BPMs for the X-FEL/SPring-8 FEL are designed for a lower resonant frequency of 4.76 GHz for both the dipole and monopole cavity, which is shifted from the accelerator RF frequency to avoid dark current. Measurements taken at the SCSS test accelerator [11] show a resolution of better than 200 nm. Additionally, the TM_{010} monopole cavity can be used to provide a timing signal from a phase measurement. The phase difference from two adjacent BPMs is shown in Fig. 3 with a width corresponding to a resolution of less than 25 fs for a single BPM.

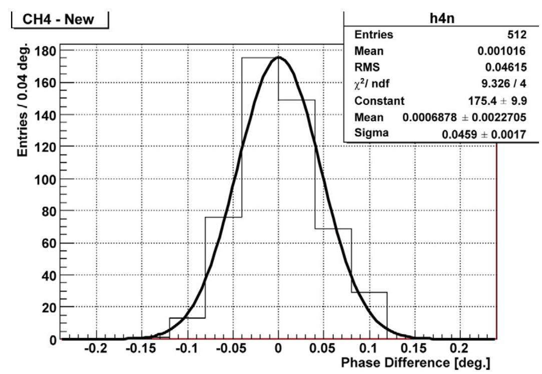

Figure 3: Phase difference between two SCSS cavity BPMs using the monopole cavity phase measurement [11].

Based on the SCSS design, the RF cavity BPMs for the E-XFEL [12] have a resonant frequency of 3.3 GHz and feature a low Q of 70 in order to resolve the beam position of the bunches within the bunch train spacing of 220 ns for the IBFB. A 10 mm aperture version for the undulator and a 40 mm one for the IBFB are designed for 1 μm resolution.

LCLS Transverse Feedback

At LCLS multiple transverse orbit feedback loops [13] are implemented as shown in the schematic in Fig. 4. The loops are mainly located at the beginning of each accelerator section as well as in the transport line to the undulator and one for the final launch into the undulator. The feedback loops operate independently from each other and nearby feedbacks are decoupled by using different time scales, e.g. the transport line feedback runs at 10 Hz, whereas the undulator launch feedback operates at 1 Hz.

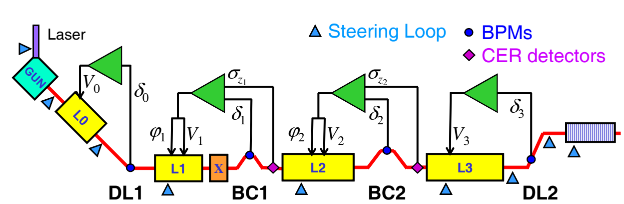

Figure 4: Schematic of the LCLS feedback system.

The feedback software measures synchronously for each bunch the beam position at several BPMs and compares this to a configurable reference orbit to calculate the required changes for upstream correctors. The response matrix is calculated from the online accelerator beam transport model. Additionally, a position and angle offset at the first BPM of each loop can be set in the control system which is useful for accelerator performance optimization.

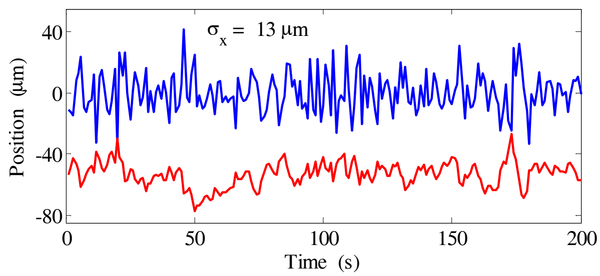

Figure 5: Launch feedback for the LCLS undulator. Shown at 6.7 GeV over 3 min are the horizontal beam position (blue) and the effective correction from the feedback (red).

An example of a feedback loop is shown in Fig. 5 for the undulator launch feedback. The feedback measures the beam position at 10 BPMs in the first 1/3 of the undulator to cover sufficient phase advance. The residual horizontal rms jitter for this measurement of 13 μm and 2 μrad at the undulator entrance is about 30-40% larger than for the vertical plane due to uncompensated horizontal dispersion in the undulator. Although this jitter at 6.7 GeV is about 25% of the beam size, the $\sigma/10$ value has been achieved with a more optimized accelerator tuning.

XFEL Orbit Intra-bunch Feedback

The long bunch trains for the E-XFEL of more than 3000 bunches and about 200 ns spacing require a fast intra-bunch feedback [14] to correct orbit changes within the bunch train and slow jitter between different macro bunches within the first part of each bunch train. A schematic of the system being developed for the XFEL is shown in Fig. 6.

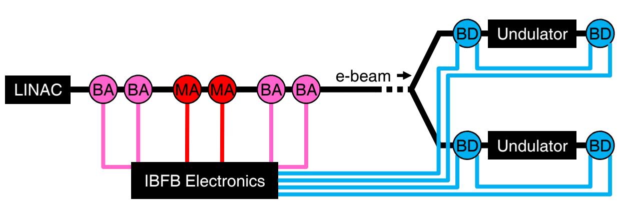

Figure 6: Schematic of the E-XFEL transverse intra-bunch feedback [15]. BA and BD are analog and digital output BPMs, MA are analog input magnets.

The beam position is measured at two downstream RF cavity BPMs which send down-mixed analog signals to the ADC of the IBFB electronics [15] for a fast latency of 1 μs. An FPGA board computes the corrections which are send to fast strip-line kickers. The two upstream RF BPMs are used for calibration of the kickers. The undulator BPMs are connected with fibers to the IBFB electronics and the signals are used for a slow feedback to correct residual errors between the IBFB location and the undulators.

LONGITUDINAL FEEDBACK

Longitudinal feedback systems regulate the amplitude and phase of the accelerating structures based on measurements of beam energy and bunch length to stabilize the electron beam energy and peak current, and hence the photon wavelength and pulse length. The diagnostics for these parameters have to be single shot and for the IBFB have to also resolve beam parameters within the bunch train.

Longitudinal Diagnostics

The most convenient fast and single shot non-interceptive bunch length measurement for bunches as short as a few μm uses coherent radiation emitted from the electron beam at wavelengths longer than the bunch length and integrated the radiation spectrum over a reasonable range to be sensitive to the bunch length. Such a signal only provides a relative measurement of the bunch length and requires some other means to calibrate. The LCLS bunch length monitors (BLM) [16] utilize coherent edge radiation (CER) emitted from the exit edge of the last chicane magnet in each bunch compressor. The radiation is separated from the electron beam with an annular mirror and then imaged onto pyroelectric detectors with low pass filters in the beam path to remove short wavelength radiation below 20 μm stemming from the fine structure of the bunch which is unrelated to the bunch length. The calibration of the detector signal is obtained from measurements of the bunch length using the transverse deflector cavity at various compression factors in the bunch compressors [13].

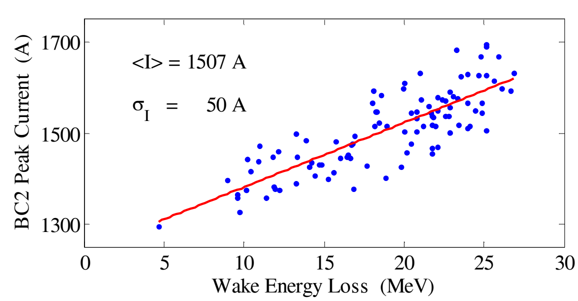

Figure 7: Correlation of LCLS bunch length monitor with wake field energy loss. The BLM noise level is 3%.

The resolution of the BLM can be estimated by a correlation with the bunch length sensitive energy loss of the electron beam in the undulator due to wake fields. This loss can be calculated for every bunch and the correlation is shown in Fig. 7 with a peak current measurement noise of

3% which is significantly lower than the stability requirement of the peak current of 10% for the LCLS.

A similar system is implemented at FLASH as a bunch compression monitor (BCM) [17] using coherent diffraction radiation from two thin metal blades close to the electron beam. The optical transport to the detector has a GHz to THz bandwidth and the fast pyroelectric detector readout provides an intra-bunch train resolved bunch length signal.

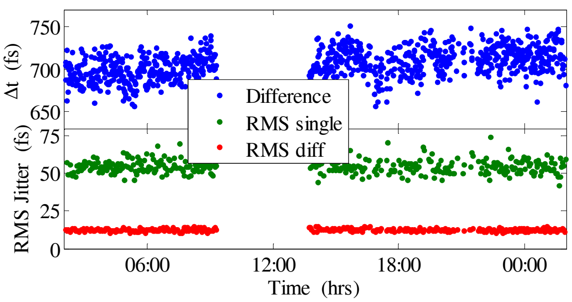

Figure 8: LCLS phase cavity signal and jitter over 24 h.

Measuring the arrival time of the electron beam after a chicane can be used for an energy feedback since the time of flight through the chicane is energy dependent. A bunch arrival monitor (BAM) [18] has been developed at FLASH which uses a 4 button pick-off to generate timing signals from the beam. The signals are compared to the fiber distributed reference laser pulses which have a stability of 6 fs due to an active fiber length stabilization system. The signal from the electron beam is encoded onto the laser amplitude with an electro-optic modulator and the laser is then sampled with a 108 MHz ADC. The system operates at the zero-crossing of the amplitude modulation to be less sensitive to laser amplitude jitter and the bunch arrival time of each bunch in the train has been measured with better than 10 fs resolution [19].

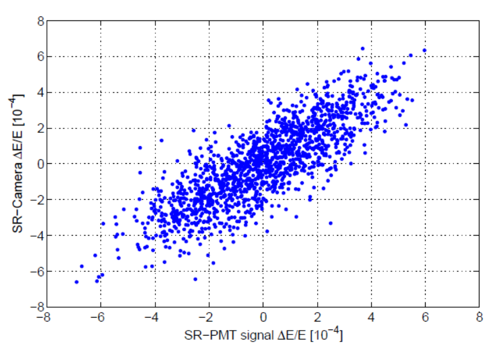

Figure 9: Resolution of the FLASH synchrotron radiation monitor [21].

The system developed at LCLS for the bunch arrival time [20] uses a monopole mode phase cavity resonant at 2805 MHz whose signal is down-mixed with the main S-band frequency at 2856 MHz and digitized with a 16 bit ADC. The 24 h performance is shown in Fig. 8 with the arrival time difference between two adjacent phase cavities and the rms jitter of a single cavity and of the difference signal. From the latter the jitter between the two cavities is obtained as 15 fs. This system is presently not used in a beam feedback, but rather to provide timing information for the user experiments for off-line analysis.

A direct energy measurement in a chicane can be done with a synchrotron radiation monitor (SRM) to measure beam size and beam position in the center of the chicane. A system used at FLASH images the synchrotron radiation from the third bend in a chicane via a beam splitter onto an ICCD and a multi-anode PMT [21]. The ICCD provides the energy spread for a single bunch out of the bunch train and the PMT signals digitized at 1 MHz give the centroid beam energy for each bunch in the train. A correlation between them is shown in Fig. 9 indicating an energy resolution of better than 10^{-4}.

LCLS Longitudinal Feedback

The schematic for the LCLS longitudinal feedback is shown in Fig. 4. It regulates the amplitude of all 4 linac sections and the phase of the two sections upstream of each bunch compressor using energy measurements after each acceleration section and the bunch length obtained after each bunch compressor. The original design [22] proposed a cascaded feedback with a 6 by 6 matrix coupling the 6 measurements to the 6 actuators which has been implemented in Matlab and operates at about 5 Hz [13]. A more recent version uses virtual actuators for energy gain and chirp of the accelerator sections to decouple the energy and bunch length feedback and the system consists of 6 loops operating independently from each other.

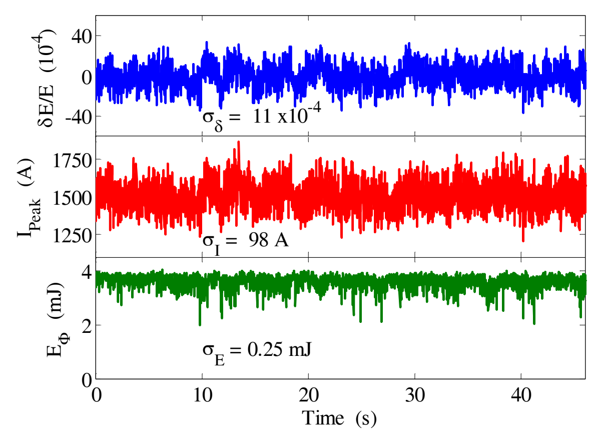

Figure 10: Performance of the LCLS longitudinal feedback over 45 s.

Figure 10 shows the feedback performance over 45 s for a 6 GeV beam. The energy is stable to 10^{-3}, the peak current jitter is 7%, and the photon pulse energy has an rms jitter of 6%. The lowest jitter achieved so far is 3%.

The planned operation of LCLS at 120 Hz requires a fast feedback system [23] which operates on EPICS IOCs on a dedicated network. The RF amplitude and phase and some of the corrector magnets are getting equipped with pulse by pulse control to compensate for different noise from the 2 interleaved 60 Hz phases of the main AC power.

FLASH Longitudinal Intra-bunch Feedback

A intra-bunch feedback system has been implemented at FLASH to regulate amplitude and phase of the first accelerating module which has the largest impact on beam energy and bunch length [19]. The input for the amplitude control is a BAM and for the phase control a BCM, both located after the second bunch compressor. The feedback is implemented as a PID loop on a FPGA based controller board. The effect of the IBFB can be seen in Fig. 11 where the arrival time jitter gets reduced from 240 fs to 40 fs rms. The rapid change at the beginning of the bunch train is from beam loading and cannot be corrected by the feedback due to the latency of the super-conducting RF of 30 μs.

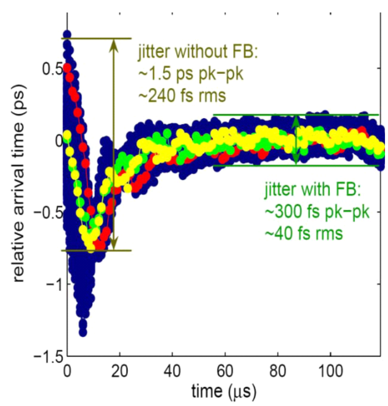

Figure 11: Intra-bunch feedback at FLASH for the arrival time [19].

A different feedback system for the intra-bunch beam energy was also tested at FLASH using the SRM and a learning feed forward algorithm to correct both stochastic and deterministic disturbances within the bunch train [24]. Figure 12 shows that the energy change along the beginning of the bunch train becomes reduced by an order of magnitude within a few iterations of the algorithm to the 10^{-3} level.

SUMMARY

State of the art diagnostics has been developed to meet the resolution requirements for stable SASE operation of X-ray FELs. Feedback systems have been successfully implemented to enable stable beam conditions for user experiments over many hours. Optical synchronization schemes enable timing measurements with around 10 fs resolution to synchronize user experiments to the accelerator.

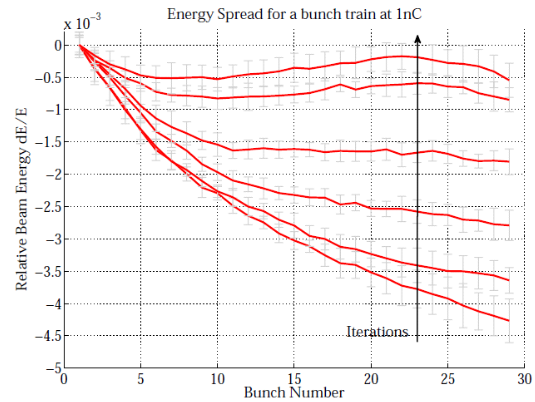

Figure 12: Feed forward algorithm for intra-bunch energy feedback at FLASH [24].

REFERENCES

[1] W. Ackermann, *et al.*, Nature Photonics 1 (2007) 366.

[2] T. Shintake, *et al.*, Nature Photonics 2 (2008) 555.

[3] P. Emma, Proceedings of PAC 2009, Vancouver, BC, May 2009, p. TH3PBI01 (2009).

[4] SCSS X-FEL Conceptual Design Report, RIKEN (2005).

[5] The European X-Ray Free-Electron Laser Technical Design Report, DESY 2006-097, DESY (2007).

[6] T. Tanaka, H. Kitamura, T. Shintake, Nucl. Instr. and Meth. A 528 (2004) 172.

[7] E. Medvedko, *et al.*, Proceedings of BIW 2008, Lake Tahoe, CA, May 2008, p. TUPTPF037 (2008).

[8] R. M. Lill, *et al.*, Proceedings of PAC 2007, Albuquerque, NM, June 2007, p. FRPMN111 (2007).

[9] P. Emma, *et al.*, Nucl. Instr. and Meth. A 429 (1999) 407.

[10] S. Smith, *et al.*, Proceedings of DIPAC 2009, Basel, Switzerland, May 2009, p. TUOC03 (2009).

[11] H. Maesaka, *et al.*, Proceedings of DIPAC 2009, Basel, Switzerland, May 2009, p. MOPD07 (2009).

[12] D. Lipka, *et al.*, Proceedings of DIPAC 2009, Basel, Switzerland, May 2009, p. MOPD02 (2009).

[13] J. Wu, *et al.*, Proceedings of FEL 2008, Gyeongju, Korea, Aug. 2008, p. MOPPH052 (2008).

[14] B. Keil, *et al.*, Proceedings of DIPAC 2007, Venice, Italy, May 2007, p. WEPB02 (2007).

[15] B. Keil, *et al.*, Proceedings of EPAC 2008, Genoa, Italy, June 2008, p. THPC123 (2008).

[16] H. Loos, *et al.*, Proceedings of PAC 2007, Albuquerque, NM, June 2007, p. FRPMS071 (2007).

[17] C. Behrens, *et al.*, these proceedings, p. MOPD090.

[18] M. K. Bock, *et al.*, Proceedings of FEL 2009, Liverpool, UK, Aug. 2009, p. WEPC66 (2009).

[19] F. Loehl, *et al.*, Proceedings of EPAC 2008, Genoa, Italy, June 2008, p. THPC158 (2008).

[20] J. Frisch, *et al.*, these proceedings, p. TUPE066.

[21] A. Wilhelm, C. Gerth, Proceedings of DIPAC 2009, Basel, Switzerland, May 2009, p. TUPD43 (2009).

[22] J. Wu, P. Emma, L. Hendrickson, Proceedings of PAC 2005, Knoxville, TN, May 2005, p. 1156 (2005).

[23] D. Fairley, *et al.*, Proceedings of ICALEPCS 2009, Kobe, Japan, Oct. 2009, p. THB001 (2009).

[24] C. Gerth, F. Ludwig and C. Schmidt, Proceedings of DIPAC 2009, Basel, Switzerland, May 2009, p. TUPD22 (2009).